Approach for early-warning collapse of double-span steel portal frames induced by fire

doi: 10.1016/j.firesaf.2022.103628

Wei Ji[1], Shaojun Zhu[1,2], Guo-Qiang Li[1,2*], Guobiao Lou[1,2], Shouchao Jiang[1,2]

[1] College of Civil Engineering, Tongji University, Shanghai 200092, China

[2] State Key Laboratory of Disaster Reduction in Civil Engineering, Tongji University, Shanghai 200092, China

[*] Corresponding author E-mail: gqli@tongji.edu.cn

Abstract

The unexpected collapse of burning buildings has posed a great threat to firefighters. Hence, early-warning methods for fire-induced collapse are urgently needed to avoid secondary casualties. This paper proposes an early-warning approach for predicting the collapse of double-span steel portal frames based on real-time measurement of displacements and displacement velocities of the burning frame. Firstly, numerical models are established to simulate the collapse behavior of double-span steel portal frames under fire, and six collapse modes of the frames are summarized through parametric analysis. The displacements and displacement velocities of the apex, eaves, and mid-span of rafters, defined as the key monitoring physical parameters (KMPPs), are found to have a close relationship with the collapse mode and time of the burning frames. Secondly, by exploring the rules of the KMPP-time curves, the characterized points that can be used for early warning of the collapse of the frame are extracted. Then, the early-warning approach applicable to six collapse modes is proposed based on the emergence of various characterized points. For universalizing the collapse prediction, early-warning time ratios are introduced and determined according to the reliability theory. Finally, the practicability and accuracy of the proposed approach are validated by an existing fire test.

Keywords

double-span steel portal frame, early warning, collapse mode, numerical simulation, fire-induced collapse

1 Introduction

Steel structures are prone to collapse under fire due to severe degradation of the material properties at elevated temperatures [1]. As the bearing capacity of heated structural components decreases with the development of the fire, localized or overall collapse of the structure occurs. The fire-induced collapse of the burning structure may bring about heavy casualties and significant social impacts, e.g., the collapse of the World Trade Center in 2001 [2]. Therefore, the fire-induced collapse of steel structures has been an important research topic in recent years. Some research focuses on fire detection to help put out the fire at its developing stage [3, 4]. Solórzano *et al.* [5] explored the performance of a gas sensor array in fire detection and found that it performed better than traditional smoke detection systems in detecting smoldering and plastic fires. Huang *et al*. [6] introduced spectral analysis in the fire image detection technology to reduce the false positive rate of convolutional neural network-based fire detection methods. Sharma *et al*. [7] suggested using the sensor network coupled with unmanned aerial vehicles to build a fire detection system in the construction of smart cities.

However, the fire detection method may have false positives or omissions. Moreover, if numerous inflammable are stacked in the building or the fire brigade encounters obstacles on the road, the fire cannot be controlled in time even if it is detected. In this case, it is necessary to guarantee the fire resistance of the structure to prevent the fire-induced collapse within a designed time, ensuring enough time for the escape of occupants and evacuation of firefighters. Shakil *et al*. [8] studied the fire response of a high-strength steel (HSS) beam and found that HSS beams have greater strength reserve compared to mild strength steel beams. Jiang *et al*. [9–11] studied the collapse resistance of steel frames under fire, considering the variation of load ratios, initial imperfection, and fire scenarios. The three-dimensional model was established and suggested to be used, as it can consider the influence of slabs and load redistributions along two spans. Yu *et al*. [12] advised increasing the crack resistance of joints to improve the collapse resistance of steel frames with the composite floor. Lu *et al*. [13] analyzed the fire performance of a steel truss roof structure considering both heating and cooling phases. They found that the water cooling near the supports can lead to structural damage, which should be considered in fire design. Du [14] explored the fire behaviors of double-layer gird structures and found that the post-buckling behavior can improve the fire resistance of the structure. Röben *et al*. [15] studied the behavior of a multi-story frame under a vertically traveling fire. They suggested that several fire spread rates should be considered in the fire-resistance design to ensure structural integrity under traveling fires.

Despite all the research findings mentioned above, fire-induced collapse accidents still occur occasionally due to unreasonable designs, delays in fire rescue, or other accidental and human errors. Therefore, it is necessary to conduct research not only on preventing fire-induced collapse but also on minimizing losses if an unexpected collapse occurs. For example, firewalls are suggested to be set between frames to prevent fire spread. Ali [16] explored the safe clearance between frames and firewalls to avoid damage to firewalls under fire due to the expansion of the heated frame. In addition, Lou *et al*. [17] highlighted that an inward collapse mode is preferred to an outward collapse mode as it can help extinguish the fire inside the burning frame and protect people outside. Further analysis indicated that frames with rigid or semi-rigid column bases are prone to inward collapse modes [18, 19]. Besides, dividing multiple fire compartments was also advised for multi-story steel frames to provide safe means of escape for occupants [20].

Recently, investigations on early-warning methods for the fire-induced collapse have received increasing attention since they are of great significance for firefighters. Firefighters are more vulnerable to fire-induced collapse as they need to rush into the burning buildings to rescue trapped occupants or put out the fire [21, 22]. However, for the time being, firefighters rely mainly on their visual observation and experience to predict the collapse in a fire scene. This inaccurate and unreliable estimation can bring great trouble to the fire brigade. On the one hand, an over-conservative evaluation of the collapse risk may lead to insufficient time for firefighters to rescue and control the fire. In contrast, an over-radical evaluation may lead to insufficient time for the evacuation of firefighters. Therefore, it is necessary to explore the real-time early-warning approach for accurately predicting the fire-induced collapse of different structural forms that are prone to collapse. For example, Jiang *et al*. [23] developed a safety monitoring system for steel truss structures. The system can evaluate the real-time status of the burning structure based on temperature data acquired from embedded sensors.

Specifically, early-warning methods for the fire-induced collapse of steel portal frames are urgently needed. Steel portal frames are widely used in industrial and commercial buildings due to their excellent spanning ability, simple design methods, and high construction efficiency [24]. However, the fire-induced collapse of steel portal frames accounts for a large number of firefighter casualties because of their high level of fire loads and low level of redundancy. Jiang *et al*. [25] divided the collapse process of steel portal frames into four stages based on displacements of the heated columns and rafters. Firefighters are advised to evacuate from the burning frame when the heated column moves back to its initial position. However, literature [25] focuses on collapse prediction under a predetermined fire scenario and determinate structural parameters, which is hard to achieve in actual firefighting. In order to address this issue, Li *et al.* [26] summarized four collapse modes of single-span steel portal frames under any fire scenarios based on the analysis of collapse mechanisms. Further analysis indicated that the collapse rules of the burning frames vary with the collapse modes. On this basis, three-level early-warning methods for different collapse modes were proposed, and the uncertainties of fire scenarios, geometric and physical parameters were considered in the quantitative collapse prediction [27]. However, the proposed early-warning methods concentrate on single-span steel portal frames. For multi-span steel portal frames, which are more predominant in practical applications, the collapse mechanisms are more complex due to an increased number of force transmission paths. Therefore, it is worth studying whether the proposed early-warning methods presented in literature [27] can be used in multi-span steel portal frames.

This study focuses on early-warning methods for the fire-induced collapse of double-span steel portal frames. The paper is organized as follows: Section 2 introduces the numerical analysis scheme, including the numerical model and the parametric analysis scheme. Based on the numerical analysis results, Section 3 summarizes the collapse modes of the frames under any fire scenarios, analyzes their corresponding collapse mechanisms, and compares the collapse modes and mechanisms with single-span steel portal frames. Section 4 investigates the variation rules of the key monitoring physical parameters (KMPPs) under fire and proposes the identification method for the collapse modes, as well as the three-level early-warning methods. Section 5 deals with the quantification of the early-warning time ratios, where the reliability theory and the Monte Carlo (MC) method are adopted. Section 6 validates the applicability of the proposed early-warning method through an existing fire test.

2 Numerical analysis scheme

2.1 Numerical model

A three-dimensional double-span steel portal frame was established in the commercial finite element program ABAQUS to simulate the collapse behavior of the frame under fire. The frame had two bays of 6 m and two spans of 24 m, as shown in Fig. 1. To represent the real frames with multiple bays, the out-of-plane rotations of the side rafters and columns of the two-bay frame system are constrained to simulate the pull force provided by adjacent non-heated bays, as shown in Fig. 2. The section information of the steel members is shown in Table 1. The Young's modulus and yield strength of steel at ambient temperature were 210 GPa and 235 MPa, respectively. The density and Poisson's ratio of steel were set as 7850 kg/m^3 and 0.3, respectively. The coefficient of thermal expansion was 1.4×10^{-5}/°C. The stress-strain model of steel at high temperatures was referred to in Eurocode 3 [28].

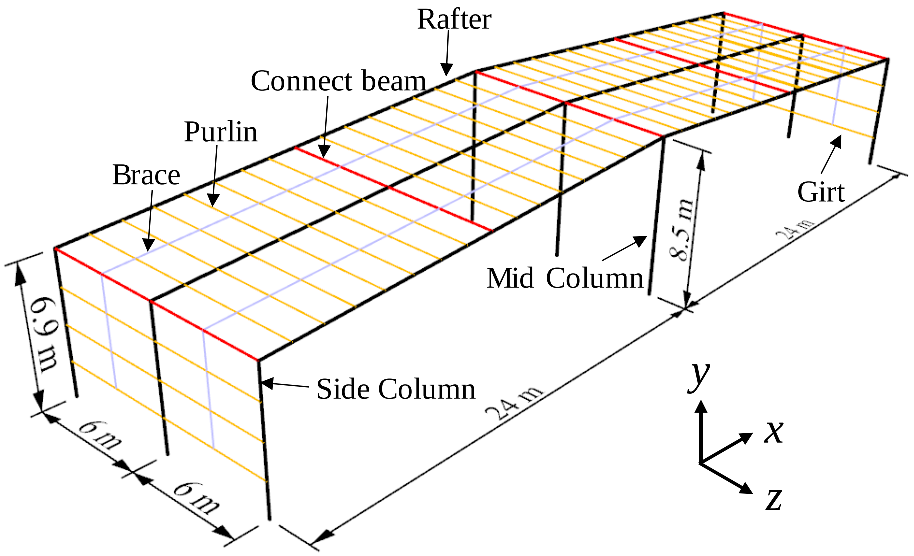

Fig. 1 Dimensions of the prototype frame.

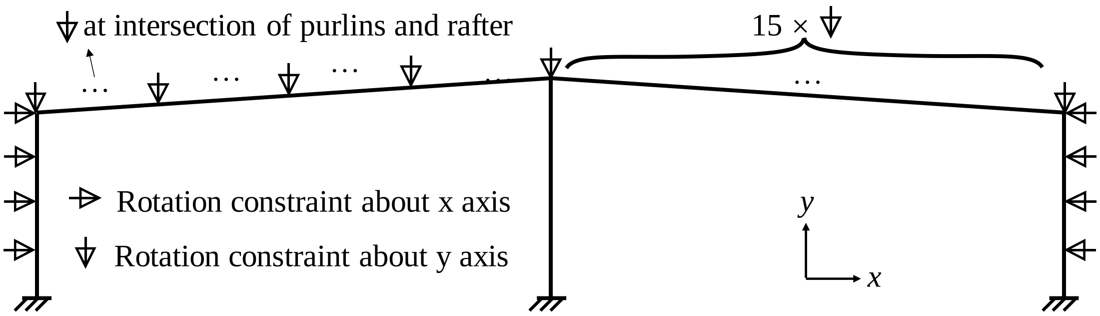

Fig. 2 Boundary conditions of the prototype frame.

Table 1 Section information of steel members.

Member type	Cross-section (unit: mm)
Side column	H550×200×6×10
Mid column	Ø273×8
Rafter	H600×200×6×8
Purlin & Girt	C200×70×20×3
Connect beam	Ø140×4.5
brace	Ø12

Two load steps were set in the finite element analysis. In step 1, dead loads were applied to the frame at ambient temperature. In this step, uniformly-distributed vertical loads were imposed on each rafter, and the load value of the middle frame was twice that of the side frame. In step 2, the frame was heated according to a parametric temperature-time curve until it collapsed. Explicit dynamic analysis is conducted to simulate the final collapse of the burning frame.

The two-node Timoshenko beam element was used to model the behavior of steel members under fire. An element mesh size of 0.15 m was used for rafters and columns, while an element mesh size of 0.3 m was used for other secondary members. The validation of the numerical model can be referred to in literature [26].

2.2 Parametric analysis scheme

Studies on collapse modes of single-span steel portal frames revealed that the collapse mode of the burning frame is related to the fire scenarios as well as geometric and physical parameters of the frame. In order to find out all the possible fire-induced collapse modes of double-span steel portal frames, as well as to explore the influencing factors of the collapse modes, the following parametric analysis scheme was adopted on the frame presented in Fig. 1:

(1) Fire scenarios

The combinations of 23 and 2 heating conditions along the span and the bay, respectively, were set to explore the effect of fire locations and power on the collapse mode. Note that each heating condition along the span is coupled with each heating condition along the bay, and the total number of fire scenarios is 23×2 = 46. The heating conditions along the span are tabulated in Table 2, where the corresponding partition numbers are defined in Fig. 3. As steel portal frames are typical large-span structures where the uniform temperature assumption of compartment fires cannot be applied, we define T1−T3 as uniform temperature partitions to consider the distance between the members and the fire. As steel members in T3 retained the ambient temperature, members in T1 and T2 would be heated to a maximum temperature of 1000 °C and 667 °C, respectively. Note that the distance between the member and the fire increases when the temperature partition varies from T1 to T3. The heating conditions along the bay are shown in Fig. 4. For heating condition H1, only the components highlighted in red, i.e., the middle bay, adjacent purlins, girts, and braces, were exposed to fire. For heating condition H2, all three bays were affected by the fire.

Table 2 Heated partitions of different heating conditions along the span.

Fire location	Heating condition	T1	T2	T3
Side column	F1	1, 2	/	3–14
	F2	1, 2	3	4–14
	F3	1–3	4	5–14
	F4	1–4	5	6–14
	F5	1–5	6, 7, 9	8, 10–14
	F6	1–6	7–10	11–14
Side span	F7	4, 5	2, 3, 6, 7, 9	1, 8, 10–14

Fire location	Heating condition	T1	T2	T3
	F8	3–6	1–2, 7–10	11–14
	F9	2–7, 9	1, 8, 10, 11	12–14
	F10	1–7, 9	8, 10, 11	12–14
	F11	1–10	11, 12	13, 14
	F12	4–6	2, 3, 7–10	1, 11–14
	F13	5–8	3, 4, 9–10	1, 2, 11–14
	F14	4–9	2, 3, 10, 11	1, 12–14
	F15	3–10	1, 2, 11, 12	13, 14
	F16	2–11	1, 12, 13	14
	F17	1–12	13, 14	/
Middle column	F18	7, 8	6, 9	1–5, 10–14
	F19	6–9	5, 10	1–4, 11–14
	F20	5–10	3, 4, 11–12	1, 2, 13, 14
	F21	4–11	2, 3, 12–13	1, 14
	F22	3–12	1, 2, 13–14	/
	F23	1–14	/	/

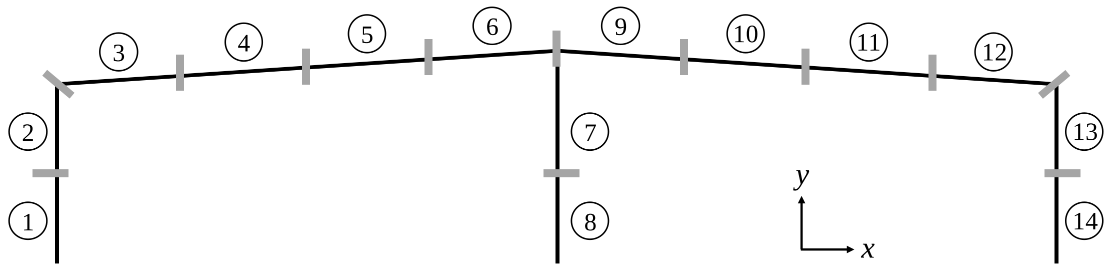

Fig. 3 Partition of steel members along the span.

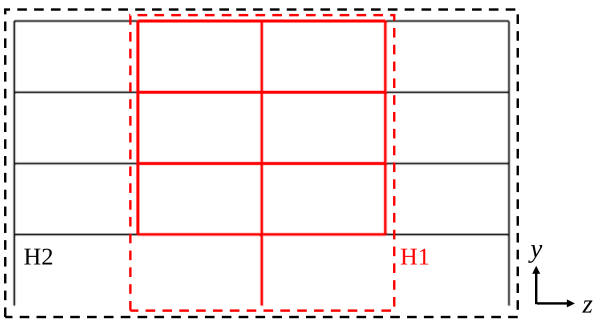

Fig. 4 Heating conditions of the frame along the bay.

(2) Fire protection

In practical engineering, steel portal frames are usually designed with a certain fire protection level to improve their fire resistance. The presence of fire protection can significantly reduce the rate of temperature increase for individual members compared to that without fire protection, thus influencing the fire response of burning frames. Five levels of fire protection were considered for rafters and columns according to Chinese code GB 50016 [29]. Note that two fire protection cases were considered for other secondary members with respect to each fire protection level, where an additional circumstance of shorter fire resistance is introduced. This is to consider the adverse effect induced by the early failure of these members, which is often observed in real fire accidents. The fire resistance time of different types of steel components is shown in Table 3. A parametric temperature-time curve was adopted for unprotected members as follows [2]:

$$T(t) = T_0 + \left(T_{\max} - T_0\right)\left(1 - \mathrm{e}^{-\alpha t}\right) \tag{1}$$

where T_0 is the ambient temperature, $T_{\max}$ is the maximum temperature of the member, t is the time, and α is a parameter indicating the heating rate. In this paper, the value of α is taken as 0.001.

A linear temperature history was assumed for the protected members for simplification [30, 31, 32], varying from the ambient temperature (20 ℃) to a predefined critical temperature (600 ℃ for beams and secondary members, 550 ℃ for columns) according to the fire resistance time of protected steel members. The temperature-time curves of rafters and columns under different fire protection levels in different temperature partitions are shown in Fig. 5.

Table 3 Fire resistance time of different fire protection levels.

Fire protection level	Fire resistance / h		
	Column	Rafter	Secondary members
1-high	3.0	2.0	2.0
1-low			1.5
2-high	2.5	1.5	1.5
2-low			1.0
3-high	2.0	1.0	1.0
3-low			0.5
4-high	0.5	0.5	0.5
4-low			No fire protection
0	No fire protection		

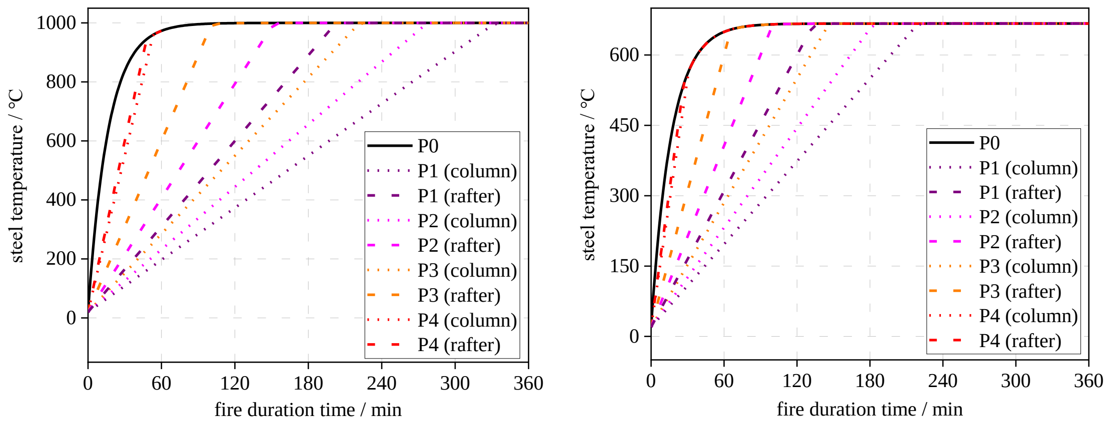

(a) steel members in T1 (b) steel members in T2

Fig. 5 Temperature curves of steel members under different fire protection levels.

(3) Cross-sectional temperature gradient

Fire tests on steel portal frames [33] found the existence of temperature gradient along the cross-sectional height of the steel member due to the heat loss from the flange exposed outdoor without fire, and the temperature gradient can be as large as 200°C when the section height was 400 mm. Therefore, four temperature gradients along the cross-section of the steel members are considered, i.e., 0, 200, 400 °C/m, and 600 °C/m.

(4) Spans

Five spans, i.e., 18, 21, 24, 27 m, and 30 m, were selected with a fixed eaves height of 6.9 m to investigate the influence of the span-to-height ratio on the collapse modes.

(5) Column spacings and braces

Three column spacings, i.e., 6, 7.5 m, and 9 m, were selected. Note that for portal frames with column spacings of 7.5 m and 9 m, roof braces were set at 1/3 and 2/3 span of the purlins in accordance with a Chinese code [34].

(6) Column bases

Two kinds of column bases, i.e., fixed and pinned, were selected.

(7) Rigidities of the top joint of the middle column

Two types of rigidity, i.e., fixed and pinned, are considered for the top joint of the middle column.

(8) Load ratios

Load ratio is defined as the ratio of the applied vertical load to the ultimate load capacity of the frame at ambient temperature. Four load ratios, i.e., 0.3, 0.4, 0.5, and 0.6, are considered.

To save the computational cost in the parametric analysis, we need to define the parameters of the basic model, where the fire protection level, cross-sectional temperature gradient, span, column spacing, and load ratio are taken as 0, 0 °C/m, 24 m, 6 m, and 0.4, respectively, with pinned column base and fixed joints for each fire scenario. For each parametric analysis in Section 3, the studied parameter will pass through all the values specified in this section, while other parameters will remain constant as mentioned above.

3 Collapse analysis of double-span steel portal frames under fire

3.1 Collapse modes and parametric effects

Collapse mode is the summary of collapse laws and reflects the collapse mechanisms of the structure under fire. Therefore, it is necessary to investigate all possible collapse modes before exploring early-warning methods. Through parametric analysis, six collapse modes were found for double-span steel portal frames under fire, namely the side-column lateral collapse mode (A), side-column buckling collapse mode (B), overall inward collapse mode (C), overall outward collapse mode (D), side-span collapse mode (E), and mid-column collapse mode (F), as shown in Fig. 6. Tables 4−10 show the effects of different parameters on the collapse modes. Note that '/' indicates that the portal frame did not collapse under the corresponding fire scenario.

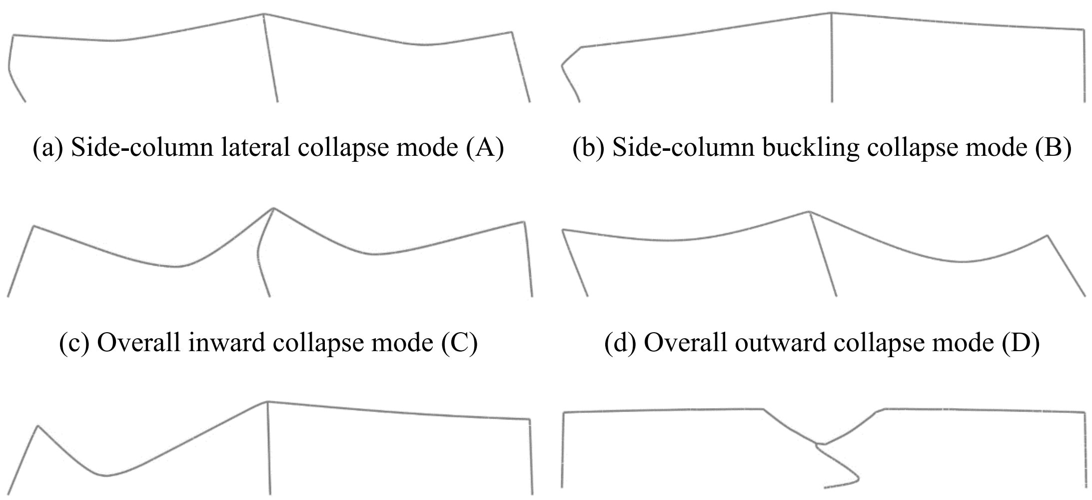

(a) Side-column lateral collapse mode (A) (b) Side-column buckling collapse mode (B)

(c) Overall inward collapse mode (C) (d) Overall outward collapse mode (D)

(e) Side-span collapse mode (E) (f) Mid-column collapse mode (F)

Fig. 6 Collapse modes of double-span steel portal frames.

Table 4 Effect of fire scenarios on collapse modes.

Scenario	Mode	Scenario	Mode	Scenario	Mode	Scenario	Mode
F1-H1	/	F7-H1	E	F12-H1	E	F18-H1	/
F2-H1	/	F8-H1	E	F13-H1	E	F19-H1	F
F3-H1	/	F9-H1	E	F14-H1	F	F20-H1	F

Scenario	Mode	Scenario	Mode	Scenario	Mode	Scenario	Mode
F4-H1	E	F10-H1	E	F15-H1	F	F21-H1	F
F5-H1	E	F11-H1	C	F16-H1	C	F22-H1	C
F6-H1	E	/	/	F17-H1	C	F23-H1	C
F1-H2	B	F7-H2	E	F12-H2	E	F18-H2	C
F2-H2	E	F8-H2	E	F13-H2	E	F19-H2	C
F3-H2	E	F9-H2	E	F14-H2	C	F20-H2	C
F4-H2	E	F10-H2	C	F15-H2	C	F21-H2	C
F5-H2	E	F11-H2	C	F16-H2	C	F22-H2	C
F6-H2	E	/	/	F17-H2	C	F23-H2	C

262 Table 5 Effect of fire protection levels on collapse modes.

Scenario	Fire protection levels								
	1-high	1-low	2-high	2-low	3-high	3-low	4-high	4-low	0
F4-H1	E	E	E	E	E	E	E	E	E
F8-H1	E	E	E	E	E	E	E	E	E
F11-H1	C	C	C	C	C	C	C	C	C
F15-H1	E	E	E	E	E	E	F	F	F
F17-H1	C	C	C	C	C	C	C	C	C
F20-H1	E	E	E	E	E	F	F	F	F
F23-H1	C	C	C	C	C	C	C	C	C
F1-H2	B	B	B	B	B	B	B	B	B
F4-H2	E	E	E	E	E	E	E	E	E
F8-H2	E	E	E	E	E	E	E	E	E
F11-H2	C	C	C	C	C	C	C	C	C
F15-H2	C	C	C	C	C	C	C	C	C
F17-H2	C	C	C	C	C	C	C	C	C
F20-H2	C	C	C	C	C	C	C	C	C
F23-H2	C	C	C	C	C	C	C	C	C

263 Table 6 Effect of cross-sectional temperature gradient on collapse modes.

Scenario	Temperature gradient (℃·m^{-1})				Scenario	Temperature gradient (℃·m^{-1})			
	0	200	400	600		0	200	400	600
F4-H1	E	E	E	E	F4-H2	E	E	E	E
F8-H1	E	E	E	E	F8-H2	E	E	E	E
F11-H1	C	C	C	C	F11-H2	C	C	C	C
F15-H1	F	F	F	F	F15-H2	C	C	C	C

Scenario	Temperature gradient (°C·m^{-1})				Scenario	Temperature gradient (°C·m^{-1})			
	0	200	400	600		0	200	400	600
F17-H1	C	C	C	C	F17-H2	C	C	C	C
F20-H1	F	F	F	F	F20-H2	C	C	C	C
F23-H1	C	C	C	C	F23-H2	C	C	C	C
F1-H2	B	B	B	B					

Table 7 Effect of span on collapse modes.

Scenario	Span (m)					Scenario	Span (m)				
	18	21	24	27	30		18	21	24	27	30
F4-H1	E	E	E	E	E	F4-H2	E	E	E	E	E
F8-H1	E	E	E	E	E	F8-H2	E	E	E	E	E
F11-H1	C	C	C	C	C	F11-H2	C	C	C	C	C
F15-H1	F	F	F	F	F	F15-H2	C	C	C	C	C
F17-H1	C	C	C	C	C	F17-H2	D	D	C	C	C
F20-H1	F	F	F	F	F	F20-H2	C	C	C	C	C
F23-H1	C	C	C	C	C	F23-H2	C	C	C	C	C
F1-H2	B	B	B	B	B						

Table 8 Effect of column spacings on collapse modes.

Scenario	Column spacing (m)			Scenario	Column spacing (m)		
	6	7.5	9		6	7.5	9
F4-H1	E	E	E	F4-H2	E	E	E
F8-H1	E	E	E	F8-H2	E	E	E
F11-H1	C	C	C	F11-H2	C	C	C
F15-H1	F	F	F	F15-H2	C	C	C
F17-H1	C	C	C	F17-H2	C	D	D
F20-H1	F	F	F	F20-H2	C	C	C
F23-H1	C	C	C	F23-H2	C	C	C
F1-H2	B	B	B				

Table 9 Effect of column base and top joint rigidity on collapse modes.

Pinned base & fixed joint		Fixed base & fixed joint		Pinned base & pinned joint	
Scenario	Mode	Scenario	Mode	Scenario	Mode
F4-S	E	F4-S	E	F4-S	E
F8-S	E	F8-S	E	F8-S	E
F11-S	C	F11-S	C	F11-S	C

Pinned base & fixed joint		Fixed base & fixed joint		Pinned base & pinned joint	
Scenario	Mode	Scenario	Mode	Scenario	Mode
F15-S	F	F15-S	F	F15-S	F
F17-S	C	F17-S	C	F17-S	C
F20-S	F	F20-S	F	F20-S	F
F23-S	C	F23-S	C	F23-S	C
F1-D	B	F1-D	B	F1-D	A
F4-D	E	F4-D	E	F4-D	E
F8-D	E	F8-D	E	F8-D	E
F11-D	C	F11-D	C	F11-D	C
F15-D	C	F15-D	C	F15-D	C
F17-D	C	F17-D	C	F17-D	D
F20-D	C	F20-D	C	F20-D	D
F23-D	C	F23-D	C	F23-D	D

Table 10 Effect of load ratio on collapse modes.

Scenario	Load ratio				Scenario	Load ratio			
	0.3	0.4	0.5	0.6		0.3	0.4	0.5	0.6
F4-H1	E	E	E	E	F4-H2	E	E	E	E
F8-H1	E	E	E	E	F8-H2	E	E	E	E
F11-H1	C	C	C	C	F11-H2	C	C	C	C
F15-H1	F	F	F	F	F15-H2	C	C	C	C
F17-H1	C	C	C	C	F17-H2	C	C	C	D
F20-H1	F	F	F	F	F20-H2	C	C	C	C
F23-H1	C	C	C	C	F23-H2	C	C	C	C
F1-H2	B	B	B	A					

From Tables 4–10, the following mechanisms can be summarized for the collapse modes:

(1) Side-column collapse modes A & B usually occur when the fire is located near the side column. At the early stage of fire, the heated eave deforms outwards and upwards due to thermal expansion. The lateral displacement of the side column will bring about an additional bending moment, which further intensifies the second-order effect. If the lateral restraint of the frame is weak (Table 9) or the vertical load is large (Table 10), the second-order effect cannot be ignored. In this case, the column will collapse laterally at elevated temperatures, and the side-column lateral collapse mode A occurs. If the lateral restraint of the frame is strong, the lateral displacement of the heated column

can be ignored. In this case, the column will buckle due to material property degradation, and the side-column buckling collapse mode B occurs.

(2) Overall collapse mode C & D usually occur in large-scale fire scenarios (Table 4). At fire ignition, the heated rafters and columns deform upwards and outwards due to thermal expansion. With the development of the fire, the rafters deform downwards due to material degradation while the columns continue to deform outwards. If the outward expansion of the heated column can be restricted, the overall inward collapse mode C occurs, in which case the side columns will be pulled inwards due to the catenary effect provided by rafters. Otherwise, the outward expansion continues until the frame collapses outwards in one direction. Parametric analyses indicated that reducing the rotational stiffness of the column base (Table 9) or increasing the column spacing (Table 8) will weaken the lateral restraints to the heated frame, thus making the overall outward collapse mode D more prone to occur. On the contrary, increasing the span will strengthen the catenary effects produced by rafters (Table 7), thus increasing the possibility of the overall inward collapse mode C.

(3) Side-span collapse mode E usually occurs when the fire is located at a single span of the frame (Table 4). The heated rafter will bend downwards and pull the side column inwards while the unheated span of the frame remains upright.

(4) Mid-column collapse mode F usually occurs when the fire is located near the mid-column (Table 4). The heated column will compress due to the applied vertical load and material degradation at elevated temperatures. Due to the tensile force provided by rafters and purlins, the structure collapses locally near the fire-affected column. Moreover, collapse mode F is more likely to occur when the frame has a low fire protection level (Table 5).

Besides, it can be concluded from Table 6 that the temperature gradient of the cross-section does not impact the final collapse mode.

From the perspective of fire rescue, an inward collapse mode is preferred to an outward collapse, as it can prevent the fire from spreading to adjacent buildings. Therefore, frames with fixed column bases, low load ratios, and low height-to-span ratios are recommended in practical design as they are prone to collapse modes B, C, E, and F under fire. In addition, a localized collapse usually does less harm than an overall collapse. Therefore, fire-resisting partitions are recommended to limit the fire within a specific area, thus avoiding the overall collapse modes.

3.2 Comparison of collapse modes between double-span and single-span steel portal frames

Li *et al.* [26] explored that single-span steel portal frames have four fire-induced collapse modes as shown in Fig. 7: Column lateral collapse mode S-A, column buckling collapse mode S-B, overall inward collapse mode S-C, and overall outward collapse mode S-D. Note that the modes mentioned above also appear in double-span steel portal frames.

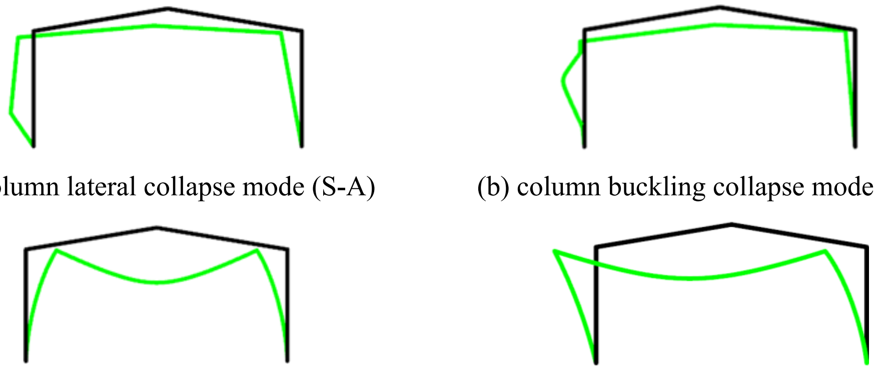

(a) column lateral collapse mode (S-A) (b) column buckling collapse mode (S-B)

(c) overall inward collapse mode (S-C) (d) overall outward collapse mode (S-D)

Fig. 7 Collapse modes of single-span steel portal frames [26].

Moreover, the existence of middle columns increases the redundancy of the frame and complicates the collapse modes of double-span steel portal frames. On the one hand, the other two columns can remain upright with only the fire-affected column failing (modes B & F). On the other hand, the cold span of the frame can serve as a restraint to the fire-affected rafters to avoid collapse (mode E). The comparison between the collapse modes of double-span and single-span steel portal frames is shown in Table 11. Since there are differences in the number of collapse modes, the early-warning methods proposed in literature [27] for single-span steel portal frames cannot be directly applied to double-span steel portal frames.

Table 11 Comparison between collapse modes of double-span and single-span steel portal frames.

<table>
<tr><th colspan="2" rowspan="2">Collapse mechanism</th><th colspan="2">Collapse mode</th></tr>
<tr><th>Double-span</th><th>Single-span</th></tr>
<tr><td colspan="2">Failure of side column</td><td>A, B</td><td>S-A, S-B</td></tr>
<tr><td rowspan="2">Large deflection of the rafter</td><td>Side column pulled inwards</td><td>C, E</td><td>S-C</td></tr>
<tr><td>Side column pushed outwards</td><td>D</td><td>S-D</td></tr>
<tr><td colspan="2">Failure of mid-column</td><td>F</td><td>/</td></tr>
</table>

4 Early-warning approach

4.1 KMPPs

The displacements and displacement velocities of the column vertex and mid-span of rafters are proved to be useful in predicting the fire-induced collapse of single-span steel portal frames. In this paper, the apex, eaves, and mid-span of the rafters are selected as monitoring positions for early warning of double-span steel portal frames.

Based on the monitoring positions, the KMPPs are displacements, as shown in Fig. 8, i.e., u_{hL}, u_{vL}, u_p, u_{hM}, u_{vM}, u_q, u_{hR}, and u_{vR}, and their corresponding displacement velocities, i.e., $\dot{u}_{hL}, \dot{u}_{vL}, \dot{u}_p, \dot{u}_{hM}, \dot{u}_{vM}, \dot{u}_q, \dot{u}_{hR}$, and $\dot{u}_{vR}$. Without loss of generality, we define the left side of the frame as the side with higher temperatures.

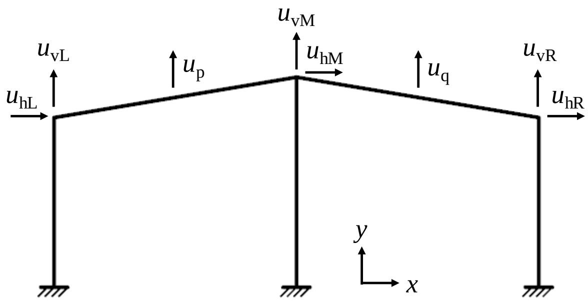

Fig. 8 KMPPs of double-span steel portal frames.

4.2 Early-warning method for each collapse mode

Based on the parametric analysis results, Fig. 9 shows the KMPP-time curves for each collapse mode under a typical parameter combination. In Fig. 9, the normalized time τ is defined as the ratio of the fire exposed time to the final collapse time. We need to note that the evolution law of the KMPPs is identical when the same collapse mode is triggered, while there is a significant difference in the evolution law of KMPPs under different collapse modes. In this way, the early-warning methods can be determined by discussing each collapse mode.

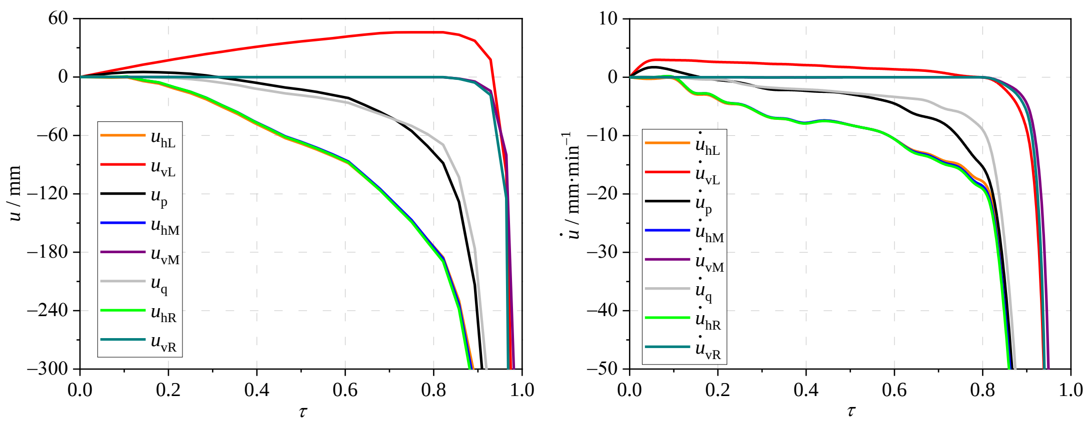

(a) Side-column lateral collapse mode A

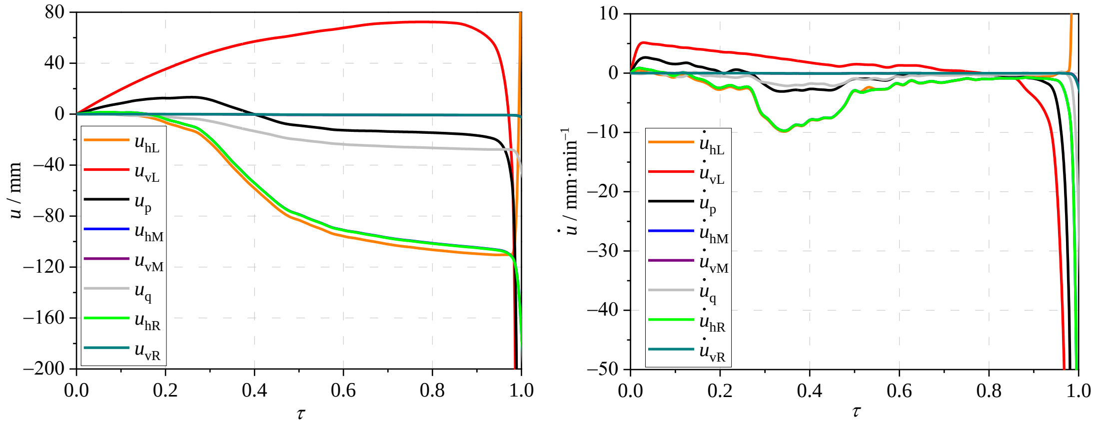

(b) Side-column buckling collapse mode B

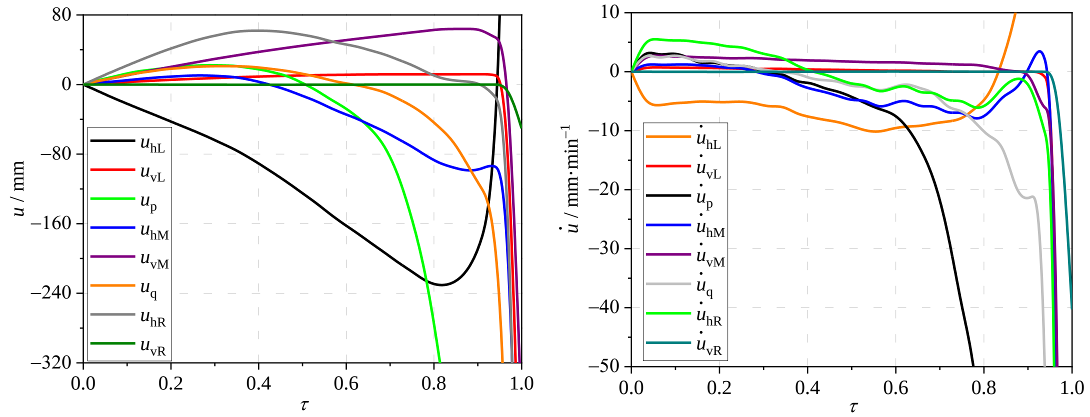

(c) Overall inward collapse mode C

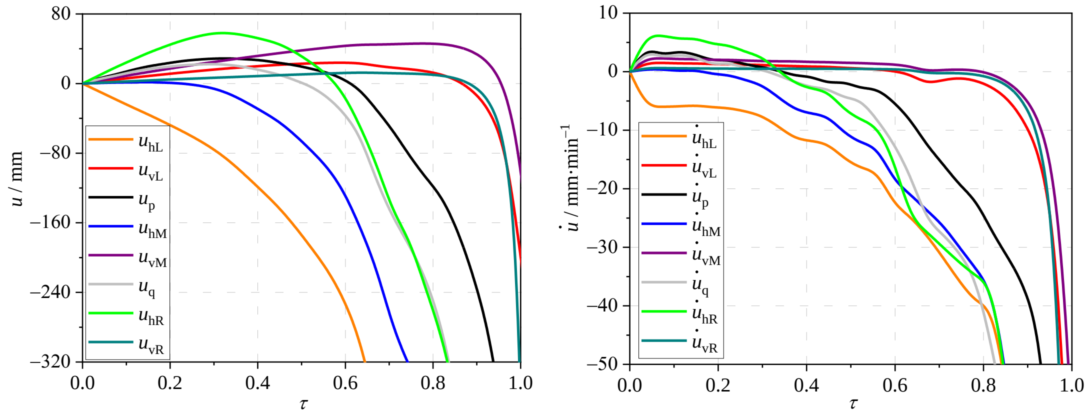

(d) Overall outward collapse mode D

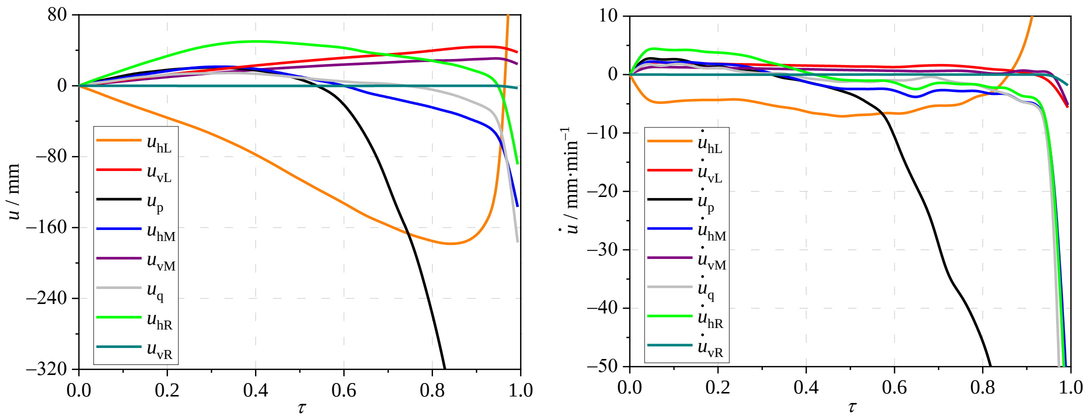

(e) Side-span collapse mode E

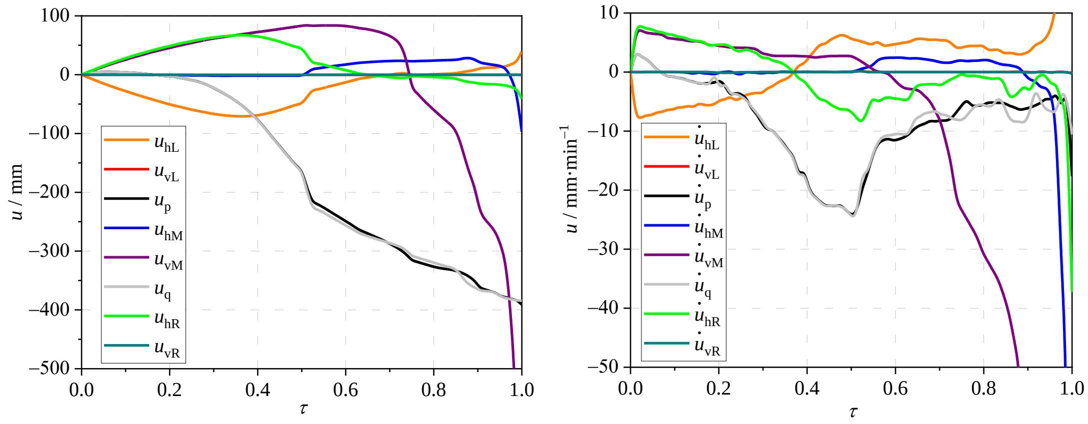

(f) Mid-column collapse mode F

Fig. 9 KMPP-time curves under typical parameter combinations for each collapse mode.

4.2.1 Collapse mode A & B

As discussed in Section 3.1, side-column lateral collapse mode A and side-column buckling collapse mode B usually occur when the fire is located near the side columns. The variation trends of KMPPs in Figs. 9(a) and 9(b) are similar to that of single-span steel portal frames, which are summarized as follows:

(1) The horizontal displacement u_{hL}, u_{hR}, and u_{hM} increase towards the fire-affected side all the time. For collapse mode A, $\dot{u}_{hL}, \dot{u}_{hR}, \dot{u}_{hM}$ increase monotonically under fire. For collapse mode B, $\dot{u}_{hL}, \dot{u}_{hR}, \dot{u}_{hM}$ increase at fire ignition and then decrease and stabilize for a long time until the frame is about to collapse.

(2) The vertical displacements u_{vL} and u_p increase firstly at the early stage of fire and then decrease with the development of the fire. For side-column lateral collapse mode A, u_{vM}, u_q, and u_{vR} decrease significantly near the collapse time, indicating an overall collapse. For side-column buckling collapse mode B, u_{vM}, u_q, and u_{vR} had little change during the fire, indicating a localized collapse.

According to the variation trends mentioned above, displacements u_p, u_{vL}, and V_{hL} and their corresponding velocities $\dot{u}_p, \dot{u}_{vL}$, and $\dot{u}_{hL}$ are selected as early-warning indexes for the collapse prediction of side-column-related collapse modes A and B. The summarized variation trends of early-warning indexes for modes A and B are shown in Figs. 10 and 11, respectively. The characteristic points with specific numerical or physical significance in these curves, namely early-warning points *A*–*D*, and *F*, were determined according to Fig. 9. The occurrence of early-warning points indicates the collapse state of the burning frame. On this basis, the three-level early-warning methods applicable to side-column-related collapse modes A and B are proposed in Tables 12 and Table 13, respectively, where the whole collapse process is divided into various stages.

The three-level early warnings represent the initial risk alert, tensional risk alert, and urgent risk alert for the possible risk of the burning frame collapse. In specific, the 1st early-warning signal indicates that the structural performance of the burning frame has been notably affected by fire, but still has enough capacity, and firefighters can devote themselves in fire rescue safely but must begin to pay attention to the risk of collapse. The 2nd early-warning signal indicates that the capacity of the frame has been seriously affected by fire, and the risk of the frame collapse increases. Firefighters should accelerate the rescue and plan the evacuation route at this stage. The 3rd early-warning signal indicates that the frame has a high possibility of sudden collapse, at which stage the firefighters must evacuate at once. Here we note again that the emergence of each early-warning level is raised by the occurrence of the corresponding early-warning point. For a certain early-warning level with multiple early-warning points, the occurrence of either (any) point will raise the early warning.

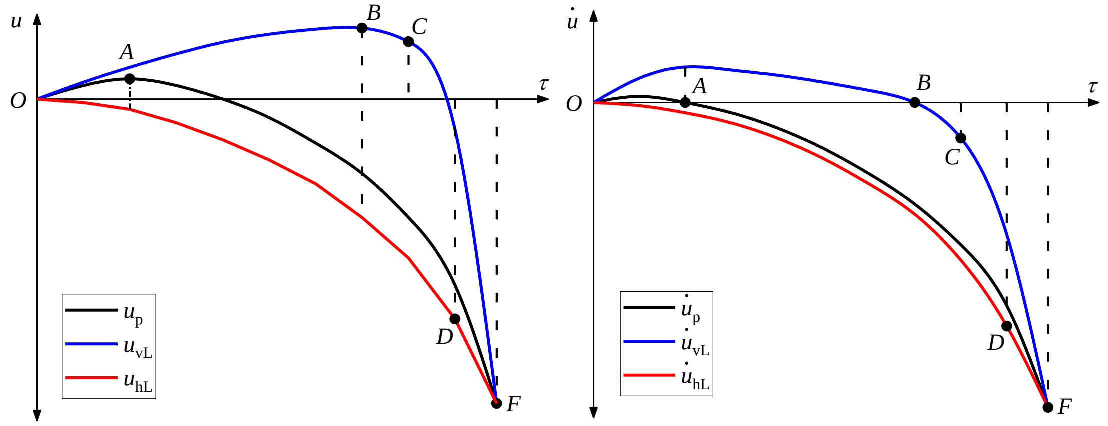

(a) displacement curve (b) displacement velocity curve

Fig. 10 Variation trends of early-warning indexes for side-column lateral collapse mode A.

Table 12 Early-warning method for side-column lateral collapse mode A.

Early-warning level	Early-warning criteria	Definition
Safe	No early-warning points occur	/
1st early-warning level	Occurrence of point *A*	*A*: u_{p} reaches its peak value
2nd early-warning level	Occurrence of point *B*	*B*: u_{vL} reaches its peak value
3rd early-warning level	Occurrence of one point *C* or *D*	*C*: $\dot{u}_{\mathrm{vL}}$ reaches -1 time of $\dot{u}_{\mathrm{vL}}^{1}$ *D*: $\dot{u}_{\mathrm{hL}}$ reaches 5 times of $\dot{u}_{\mathrm{hL}}^{1,2}$
Collapse	Occurrence of point *F*	*F*: u_{hL} reaches 1/5 of the eave height
Definitions:		

$\dot{u}_{\mathrm{vL}}^{1}$: $\dot{u}_{\mathrm{vL}}$ at 1st early-warning level

$\dot{u}_{\mathrm{hL}}^{1,2}$: average value of $\dot{u}_{\mathrm{hL}}$ from 1st early-warning level to 2nd early-warning level

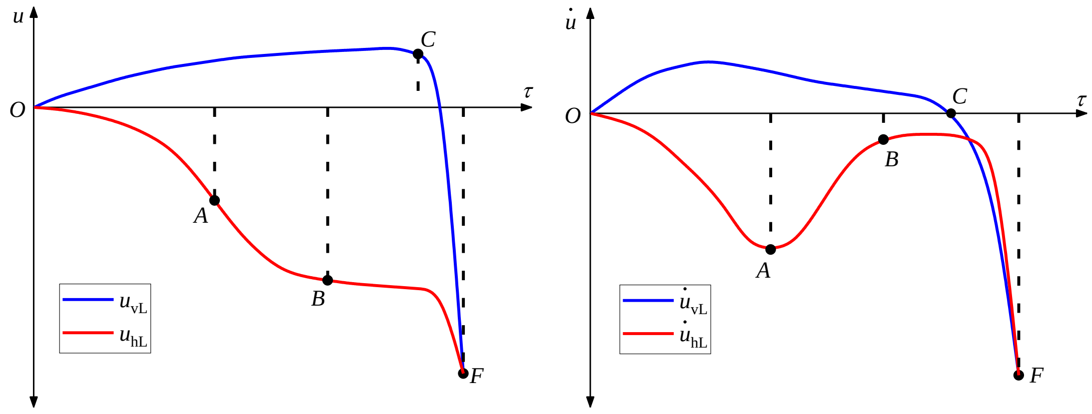

(a) displacement curve (b) displacement velocity curve

Fig. 11 Variation trends of early-warning indexes for side-column buckling collapse mode B.

Table 13 Early-warning method for side-column buckling collapse mode B.

Early-warning level	Early-warning criteria	Definition of early-warning points
Safe	No early-warning points occur	/
1st early-warning level	Occurrence of point *A*	*A*: $\dot{u}_{\mathrm{hL}}$ reaches its peak value
2nd early-warning level	Occurrence of point *B*	*B*: $\dot{u}_{\mathrm{hL}}$ decreases to 3/5 of $\dot{u}_{\mathrm{hL}}^{1}$
3rd early-warning level	Occurrence of point *C*	*C*: u_{vL} reaches its peak value
Collapse	Occurrence of point *F*	*F*: u_{hL} reaches 1/5 of the eave height

Definition:

$\dot{u}_{\mathrm{hL}}^{1}$: $\dot{u}_{\mathrm{hL}}$ at 1st early-warning level

4.2.2 Collapse modes C, D, and E

As discussed in Section 3.1, overall inward collapse mode C, overall outward collapse mode D, and side-span collapse mode E usually occur when both rafters and columns are exposed to fire. The change laws of monitoring parameters were similar to the overall collapse modes of single-span steel portal frames, which are summarized as follows:

(1) Horizontal displacements u_{hL} and u_{hR} increase outwards at fire ignition. For overall inward collapse mode C and side-span collapse mode E, u_{hL} moves inwards at the later stage of fire. For overall outward collapse mode D, u_{hL} moves outwards monotonically until the frame collapses.

(2) Vertical displacements u_{p} and u_{q} move upwards firstly due to thermal expansion, then move downwards due to material degradation. For overall

collapse modes C and D, u_{vL} and u_{vM} decrease significantly when the frame is about to collapse, indicating the failure of the fire-exposed columns. For side-span collapse mode E, u_{vM} and u_{vR} remain stable under fire, and u_q does not experience a large decrease when the frame collapses, indicating the safety of the right span of the frame.

According to the variation trends mentioned above, displacements u_p, u_{vM}, u_{vL}, and V_{hL}, and their corresponding velocities $\dot{u}_p, \dot{u}_{vM}, \dot{u}_{vL}$, and $\dot{u}_{hL}$ are chosen as early-warning indexes for the collapse prediction of modes C, D, and E. The variation trends of early-warning indexes for each collapse mode are shown in Fig. 12. Similarly, the three-level early-warning method is proposed in Table 14 for these collapse modes.

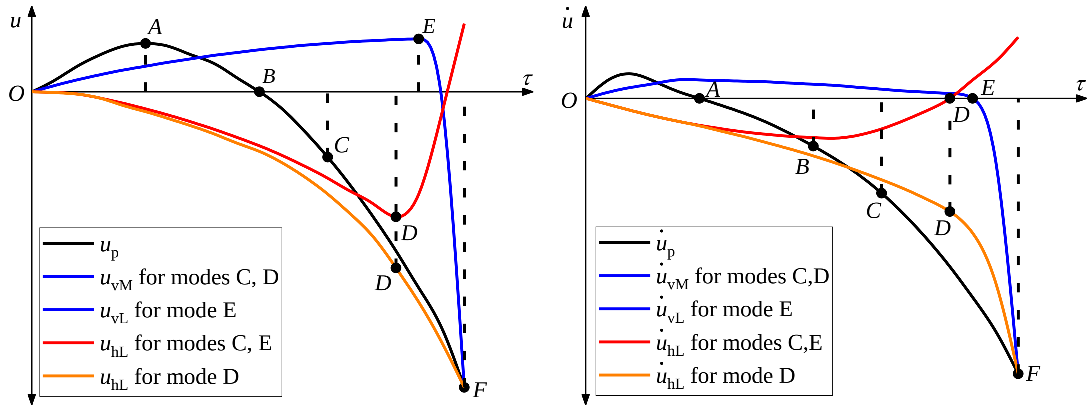

(a) displacement curve (b) displacement velocity curve

Fig. 12 Variation trends of early-warning indexes for collapse modes C, D & E.

Table 14 Early-warning method for collapse modes C, D & E.

Early-warning level	Early-warning criteria	Definition of early-warning points
Safe	No early-warning points occur	/
1st early-warning level	Occurrence of point *A*	*A*: u_p reaches its peak value
2nd early-warning level	Occurrence of one point *C*, *D* or *E*	*B*: u_p decreases to 0 *C*: $\dot{u}_p$ reaches 10 times of $\dot{u}_p^{A,B}$ *D*: u_{hL} reaches its peak value (collapse modes C and E) or $\dot{u}_{hL}$ reaches 10 times of $\dot{u}_{hL}^{A,B}$ (collapse mode D)
3rd early-warning level	Occurrence of two points *C*, *D*, *E*	*E*: u_{vM} reaches its peak value (collapse modes C and D) or u_{vL} reaches its peak value (collapse mode E)
Collapse	Occurrence of point *F*	*F*: u_p reaches 1/10 of span

Definitions:

$\dot{u}_p^{A,B}$: average value of $\dot{u}_p$ from point *A* to point *B*

$\dot{u}_{hL}^{A,B}$: average value of $\dot{u}_{hL}$ from point *A* to point *B*

4.2.3 Collapse mode F

As discussed in Section 3.1, mid-column collapse mode usually occurs when the fire is localized to the mid-column. The change laws of monitoring parameters were concluded below:

(1) Horizontal displacements u_{hL} and u_{hR} increase outwards at fire ignition and then move inwards after their peak values, while V_{hM} hardly varies until the mid-column is about to fail.

(2) Vertical displacements u_p and u_q decrease monotonically during the fire and retain below 500 mm when the frame collapses. Besides, u_{vL} and u_{vR} also remain stable under fire. u_{vM} increases at fire ignition due to thermal expansion and then decreases with the development of the fire; the final decrease is sharp since the mid-column fails due to material degradation. The aforementioned variation trends indicate that the collapse is localized near the mid-column.

According to the variation trends mentioned above, displacements u_{hL}, u_{hM}, and u_{vM}, and their corresponding velocities $\dot{u}_{hL}, \dot{u}_{hM}$, and $\dot{u}_{vM}$ are chosen as early-warning indexes for collapse prediction of the mid-column collapse mode F. The variation trends of early-warning indexes are shown in Fig. 13, and the three-level early-warning method is proposed in Table 15.

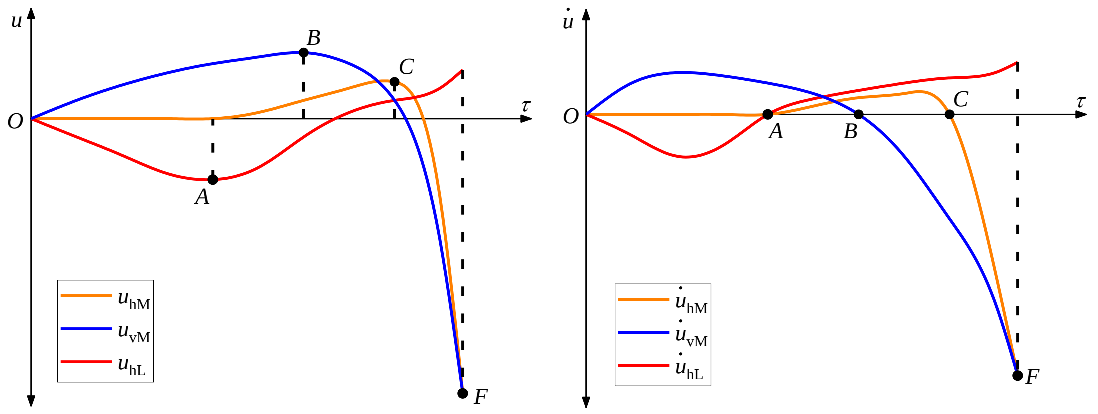

(a) displacement curve (b) displacement velocity curve

Fig. 13 Variation trends of early-warning indexes for mid-column collapse mode F.

Table 15 Early-warning method for mid-column collapse mode F.

Early-warning level	Early-warning criteria	Definition of early-warning points
Safe	No early-warning points occur	-
1st early-warning level	Occurrence of point *A*	*A*: u_{hL} reaches its peak value
2nd early-warning level	Occurrence of point *B*	*B*: u_{vM} reaches its peak value
3rd early-warning level	Occurrence of point *C*	*C*: u_{hM} reaches its peak value

Early-warning level	Early-warning criteria	Definition of early-warning points
Collapse	Occurrence of point F	F: u_{vM} reaches 1/10 of span

4.3 Identification method of the collapse mode

In Section 4.2, the three-level early-warning methods are proposed for predicting the fire-induced collapse of double-span steel portal frames. However, the proposed methods are dependent on the collapse modes. Therefore, it is essential to identify the collapse mode of the burning frame before adopting the early-warning method for collapse prediction. By comparing the variation trends of KMPPs shown in Figs. 9–13, several laws can be concluded as follows:

(1) At the early stage of fire, for collapse modes A and B, u_p is smaller than u_{vL} and u_{hL}, u_{hR} both move towards the same direction. While for collapse modes C, D, E, and F, the relationships mentioned above are completely reversed;

(2) For collapse mode A, $\dot{u}_{hL}$ increases monotonically until the frame collapses. While for collapse mode B, $\dot{u}_{hL}$ increases firstly, then decreases to a stable value, and increases again when the frame is about to collapse.

(3) For collapse mode E, u_{vM} is smaller than u_{vL}. While for collapse modes C, D, and F, u_{vM} is larger than u_{vL}.

(4) For collapse mode C and D, u_{hL} and u_{hR} have the same variation trend. While for collapse mode E, u_{hL} and u_{hR} have the opposite variation trend.

(5) For collapse mode C, u_{hL} moves inward after its peak value. While for collapse mode D, u_{hL} moves outward continuously until the frame collapses.

Based on these laws, the identification method for collapse modes of double-span steel portal frames is proposed in Fig. 14.

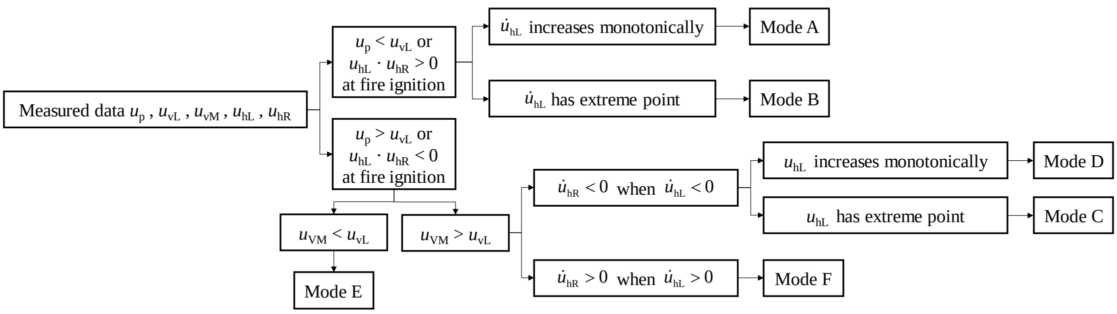

Fig. 14 Identification method for collapse modes.

5 Prediction of remaining collapse time

5.1 Determination method for two time ratios

Quantitative prediction of the collapse time during fire rescue can give firefighters a clear understanding of the collapse risk and facilitate wiser decisions. For this purpose, we introduce the early-warning time ratio t_i^{E} and the remaining time ratio t_i^{R} for collapse prediction, where the subscript i indicates the early-warning level. At each early-warning level, t_i^{E} is defined as the ratio of the early-warning time to the final collapse time, while t_i^{R} is defined as the ratio of the remaining time over the early-warning time, as illustrated in Fig. 15. Note that the time ratios can be calculated and stored in advance, and the early-warning time can be determined at the fire rescue scene according to the early-warning methods presented in Section 4.2, i.e., the remaining time T_i^{R} can be calculated by

$$T_i^{\mathrm{R}} = T_i^{\mathrm{E}} \times \left(\frac{1}{t_i^{\mathrm{E}}} - 1 \right) \tag{2}$$

or

$$T_i^{\mathrm{R}} = T_i^{\mathrm{E}} \times t_i^{\mathrm{R}} \tag{3}$$

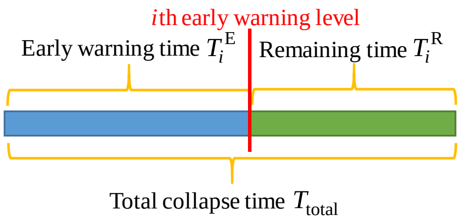

Fig. 15 Definition of the two time ratios [27].

However, some parameters of the burning frame, such as fire scenarios and load ratios, are hard to acquire real-timely at the fire rescue scene. Hence, it is difficult and time-consuming to use an accurate early-warning time ratio for collapse prediction in reality. Therefore, the reliability theory is adopted herein to consider the uncertainties of different parameter combinations. In this way, the early-warning and remaining time ratios can be determined under a certain reliability level, and the remaining time of the burning frame at the ith early-warning level can be assumed to be no less than T_i^{R}, which can be calculated according to Eq. (2) or (3). The MC method is used to consider random parameter combinations in order to determine the early-warning time ratios.

The MC samples of each collapse mode were determined according to parametric analysis. According to Section 3.1, the collapse modes are influenced by several parameters, and it is difficult to determine the accurate range of each parameter for a certain collapse mode. Therefore, the MC samples shown in Table 16 are designed to cover all the possible parameter combinations of a certain (desired) collapse mode. It is notable that the parameter combination will be excluded if an undesired collapse mode is obtained since Table 16 is roughly designed according to the parametric analysis results.

Table 16 Samples in MC method.

Influencing parameter	Collapse mode				
	A	B	C & D	E	F
Heating condition along span	{F1}	{F1}	[F2, F23]	[F2, F13]	{F14, F15, [F19, F21]}
Heating condition along bay	{H1, H2}	{H1, H2}	{H1, H2}	{H1, H2}	{H1}
Stiffness of column base	Pinned	Pinned& Fixed	Pinned & Fixed	Pinned & Fixed	Pinned & Fixed
Connection of mid column and rafters	Pinned	Fixed	Pinned & Fixed	Pinned & Fixed	Pinned & Fixed
Fire protection	9 levels				
Cross-sectional temperature gradient	[0, 600] ℃/m				
Span	{18, 21, 24, 27, 30} m				
Bay	{6, 7.5, 9} m				
Load ratio	[0.3, 0.6]				

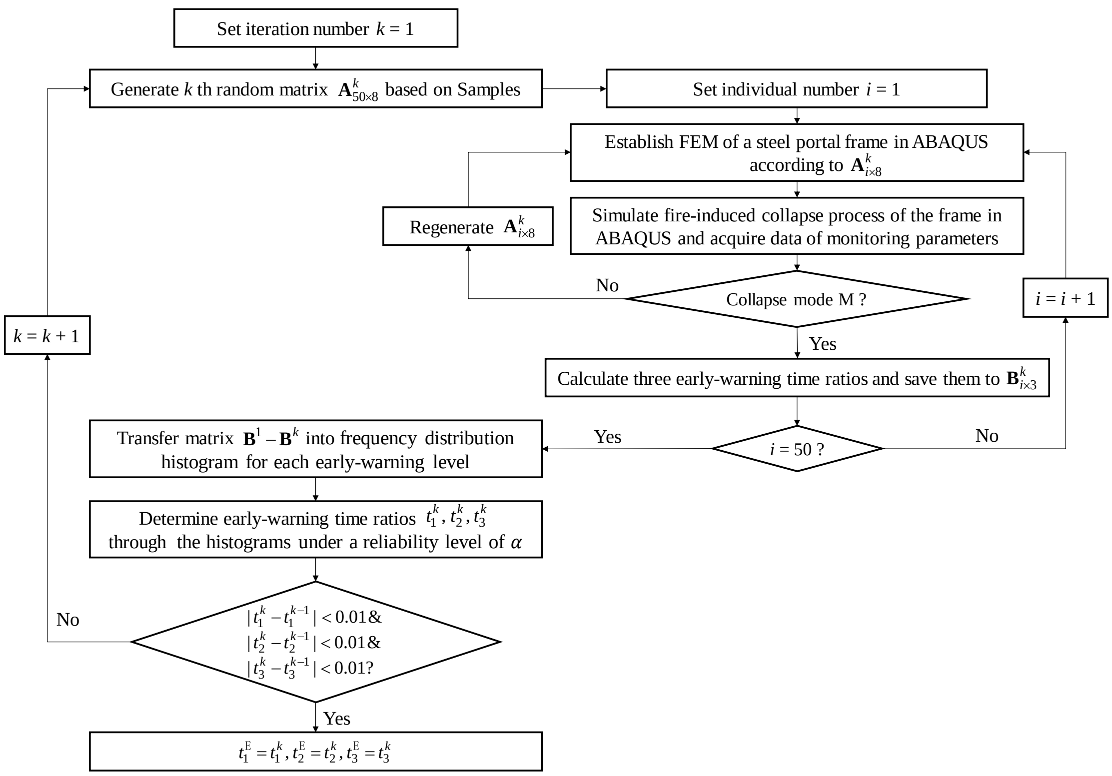

Fig. 16 Calculation method for early-warning time ratios.

For a certain collapse mode M ($M \in \{A, B, C, D, E, F\}$) with a reliability level of α, the early-warning time ratios are calculated according to the flow chart shown in Fig. 16. Readers can refer to literature [27] for a more detailed description of this method.

5.2 Quantitative collapse prediction based on reliability theory

Table 17 shows the early-warning time ratios and remaining time ratios at three early-warning levels for six collapse modes of double-span steel portal frames. It is worth noticing that the time ratios of overall inward and overall outward collapse modes were considered together as these two modes cannot be distinguished in the 1st or 2nd early-warning level due to similar early-warning points.

Table 17 Early-warning time ratios and collapse time ratios for each collapse mode under different reliability levels.

Mode	α	T_1^E	T_1^R	T_2^E	T_2^R	T_3^E	T_3^R
	30%	0.18	4.556	0.69	0.449	0.85	0.176
	40%	0.2	4.000	0.72	0.389	0.87	0.149
	50%	0.22	3.545	0.73	0.370	0.88	0.136
A	60%	0.23	3.348	0.75	0.333	0.89	0.124
	70%	0.25	3.000	0.78	0.282	0.9	0.111
	80%	0.3	2.333	0.82	0.220	0.92	0.087
	90%	0.35	1.857	0.85	0.176	0.93	0.075
	30%	0.42	1.381	0.5	1.000	0.84	0.190
	40%	0.48	1.083	0.6	0.667	0.86	0.163
	50%	0.49	1.041	0.64	0.563	0.87	0.149
B	60%	0.49	1.041	0.68	0.471	0.88	0.136
	70%	0.49	1.041	0.69	0.449	0.89	0.124
	80%	0.5	1.000	0.71	0.408	0.91	0.099
	90%	0.5	1.000	0.73	0.370	0.92	0.087
	30%	0.35	1.857	0.56	0.786	0.77	0.299
	40%	0.4	1.500	0.59	0.695	0.81	0.235
	50%	0.43	1.326	0.61	0.639	0.84	0.190
C, D	60%	0.45	1.222	0.64	0.563	0.85	0.176
	70%	0.48	1.083	0.67	0.493	0.87	0.149
	80%	0.51	0.961	0.7	0.429	0.9	0.111
	90%	0.55	0.818	0.74	0.351	0.93	0.075
E	30%	0.33	2.030	0.58	0.724	0.71	0.408
	40%	0.36	1.778	0.62	0.613	0.76	0.316

Mode	α	T_1^{E}	T_1^{R}	T_2^{E}	T_2^{R}	T_3^{E}	T_3^{R}
	50%	0.4	1.500	0.64	0.563	0.8	0.250
	60%	0.43	1.326	0.66	0.515	0.83	0.205
	70%	0.47	1.128	0.69	0.449	0.86	0.163
	80%	0.52	0.923	0.73	0.370	0.88	0.136
	90%	0.57	0.754	0.78	0.282	0.9	0.111
	30%	0.35	1.857	0.65	0.538	0.83	0.205
	40%	0.39	1.564	0.68	0.471	0.85	0.176
	50%	0.42	1.381	0.7	0.429	0.87	0.149
F	60%	0.44	1.273	0.72	0.389	0.88	0.136
	70%	0.48	1.083	0.75	0.333	0.9	0.111
	80%	0.52	0.923	0.79	0.266	0.92	0.087
	90%	0.57	0.754	0.84	0.190	0.95	0.053

6 Validation

As most fire tests on steel portal frames focused on single-span, literature [33] reported a fire test on a full-scale 36 m × 12 m double-span steel portal frame, as shown in Fig. 17. The frame failed at about 15 min after the fire ignition, as shown in Fig. 18. The heated rafters and mid columns had large downward deflections and pulled side columns inside, which aligns well with the overall inward collapse mode (collapse mode C). The vertical displacement of the heated column, vertical displacement of the heated rafter, and the horizontal displacement of a side column, were measured during the fire test, as shown in Table 17.

Fig. 17 Fire test on a double-span steel portal frame [33].

(a) during test (b) after test

Fig. 18 Collapse behavior of the test frame [33].

As shown in Fig. 19, the vertical displacement of the heated rafter reached its peak at about 7.5 min. Therefore, the first early warning was given at this time, according to Table 14. Then, the horizontal displacement of the side column reached its peak value at about 11.5 min, where the second early warning was given. Finally, the vertical displacement of the heated column reached its peak at about 15 min, and the third early warning was given. From Fig. 19, it can be observed that the heated column did not fail at 15.5 min as u_{vm} is relatively small at 15.5 min. Therefore, the final collapse time, i.e., 15 min, stated in literature [33], is not accurate, and 16 min was considered as the actual collapse time of the test frame hereinafter.

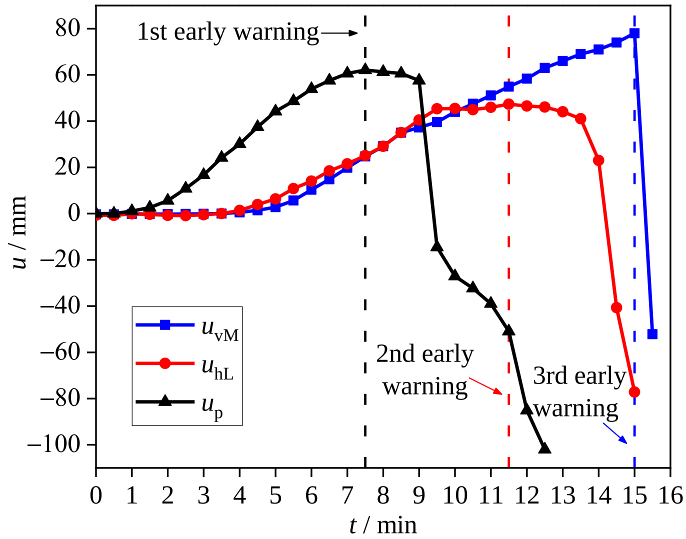

Fig. 19 Measured displacement of the test frame [33].

The remaining time of the test frame can be calculated according to Eq. (3) and Table 17 at each early-warning level. Besides, the actual remaining time of the test frame can be acquired by subtracting each early-warning time from the final collapse time, i.e., 16 min. The comparison of the calculated remaining time T_i^{R} at different reliability levels against the actual remaining time is shown in Fig. 20.

When the reliability level α is low, the calculated remaining time is far larger than the real remaining time, and the burning frame will collapse unexpectedly and cause casualties. In contrast, the calculated remaining time is smaller than the real remaining time when α is high, and the firefighters can evacuate timely before the collapse. However, an ultra-high α is not recommended since it will waste valuable fire rescue time. As shown in Fig. 20, early-warning methods with a reliability level of 70% to 80% can predict the collapse time well for this fire test.

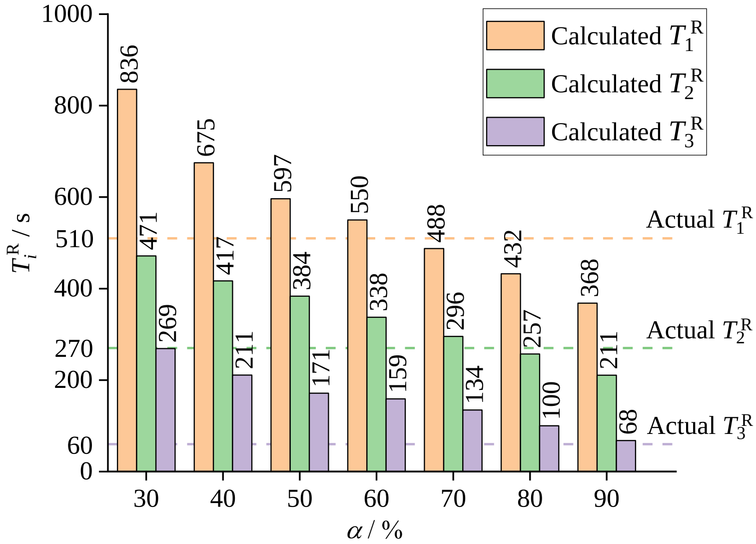

Fig. 20 Comparison of calculated and actual remaining time at each early-warning level.

7 Conclusions

This paper presented a practical way for firefighters to evaluate the collapse risk of double-span steel portal frames under fire. Collapse mechanisms of the burning frames were investigated, and six collapse modes were summarized through parametric analysis. Three-level early-warning methods based on variation trends of KMPPs were proposed for each collapse mode. Early-warning and remaining time ratios were introduced and determined based on the reliability theory for quantitative collapse prediction. The findings can be concluded as follows:

(1) Double-span steel portal frames subjected to fire may fail by side-column lateral collapse mode, side-column buckling collapse mode, overall inward collapse mode, overall outward collapse mode, side-span collapse mode, or mid-column collapse mode. Differences in collapse modes compared with single-span steel portal frames are caused by the existence of the mid-column.

(2) An inward, localized collapse is preferred to an outward, overall collapse. In this case, fixed column bases, low load ratios, and low height-to-span ratios are advised to avoid the latter collapse modes. Setting fire-resisting partitions are also suggested to limit the fire spreading.

(3) Apex, eaves, and mid-span of rafters are key positions of double-span steel portal frames under fire, which is similar to that of single-span steel portal frames. The displacements and displacement velocities of these positions in fire, defined as KMPPs, can be used to identify the collapse modes and predict the collapse time of the burning frame.

(4) Early-warning time for the collapse of a double-span steel portal frame agrees well with the test result when the reliability level is selected as 70% to 80%.

If one hopes to apply the proposed method at practical fire scenes, an integrated early-warning system should be developed for pre-storing the early-warning algorithms, measuring the real-time KMPPs, automatically analyzing the measured data, and automatically sending messages, including the early-warning level and the predicted remaining collapse time. The development of the system will be included in our future study.

Data Availability Statement

Some or all data, models, or codes that support the findings of this study are available from the corresponding author upon reasonable request.

References

[1] Y. C. Wang, T. Lennon, D. B. Moore. The behavior of steel frames subject to fire. Journal of Constructional Steel Research, 1995, 35: 291-322.

[2] A. S. Usmani, Y. C. Chung, J. L. Torero. How did the WTC towers collapse: a new theory, Fire Safety Journal, 2003, 38: 501-503.

[3] A. Gaur, A. Singh, A. Kumar, *et al*. Fire sensing technologies: a review. IEEE Sensors Journal, 2019, 19(9): 3191-3202.

[4] F. Bu, M. S. Gharajeh. Intelligent and vision-based fire detection systems: A survey. Image and Vision Computing, 2019, 91: 103803.

[5] A. Solórzano, J. Eichmann, L. Fernández. Early fire detection based on gas sensor arrays: Multivariate calibration and validation. Sensors and Actuators. B: Chemical, 2022, 352(1): 130961.

[6] L. Huang, G. Liu, Y. Wang, H. Yuan, T. Chen. Fire detection in video surveillances using convolutional neural networks and wavelet transform. Engineering Applications of Artificial Intelligence, 2022, 110: 104737.

[7] A. Sharma, P. K. Singh, Y. Kumar. An integrated fire detection system using IoT and image processing technique for smart cities. Sustainable Cities and Society, 2020, 61: 102332.

[8] S. Shakil, W. Lu, J. Puttonen. Response of high-strength steel beam and single-stroey frames in fire: Numerical simulation. Journal of Constructional Steel Research, 2018, 148: 551-561.

[9] J. Jiang, G. Q. Li, A. S. Usmani. Progressive collapse mechanisms of steel frames exposed to fire. Advances in Structural Engineering, 2014, 17(3): 381-398.

[10] J. Jiang, L. M. Jiang, *et al*. OpenSees software architecture for the analysis of structures in fire. Journal of Computing in Civil Engineering, 2015, 29(1): 04014030.

[11] J. Jiang, G. Q. Li. Progressive collapse analysis of 3D steel frames with concrete slabs exposed to localized fire. Engineering Structures, 2017, 149: 21-34.
[12] M. Yu, X. X. Zha, J. Q. Ye. The influence of joints and composite floor slabs on effective tying of steel structures in preventing progressive collapse. Journal of Constructional Steel Research, 2010, 66: 442-451.
[13] L. Lu, G. Yuan, Z. H. Huang, Q. J. Shu, Q. Li. Performance-based analysis of large steel truss roof structure in fire. Fire Safety Journal, 2017, 93: 21-38.
[14] Y. Du. Fire behaviors of double-layer grid structures under a new temperature-time curve. Procedia Engineering, 2017, 210: 605-612.
[15] C. Röben, M. Gillie, J. Torero. Structural behavior during a vertically travelling fire. Journal of Constructional Steel Research, 2010, 66: 191-197.
[16] H. M. Ali, P. E. Senseny, R. L. Alpert. Lateral displacement and collapse of single-story steel frames in uncontrolled fire, Engineering Structures, 2004, 26: 593-607.
[17] G. B. Lou, C. H. Wang, J. Jiang, *et al*. Fire tests on full-scale steel portal frames against progressive collapse, Journal of Constructional Steel Research, 2018: 145 137-152.
[18] Y. Y. Song. Analysis of industrial steel portal frames under fire conditions (PhD Thesis), University of Sheffield, UK, 2008.
[19] M Rahman, J B.P. Lim, Y Xu, *et al*. Effect of column base strength on steel portal frames in fire, Structures and Buildings, 2012, 166 (4): 197-216.
[20] R. Egle, E. R. Jamal. A study on the effect of compartment fire on the behavior of multi-storey steel frames structures, Fire Technology, 2015, 51: 867-886.
[21] L. R. Jiang, Q. L. Zhang, J. X. Shi, Y. Li. Statistic study on sacrifices of firefighters in China, Procedia Engineering, 2012, 45: 700-704.
[22] R. Kang, G. Fu, J. Yan. Analysis of the case of fire fighters casualties in the building collapse, Procedia Engineering, 2016, 135: 343-348.
[23] S. C. Jiang, S. J. Zhu, X. N. Guo, C. Chen, Z. Y. Li. Safety monitoring system of steel truss structures in fire, Journal of Constructional Steel Research, 2020, 172: 106216.
[24] SCI. Single Storey Steel Framed Buildings in Fire Boundary Conditions, Steel Construction Institute (SCI), Publication P313, Berkshire, UK, 2002.
[25] J. Jiang, C. H. Wang, G. B. Lou, G. Q. Li. Quantitative evaluation of progressive collapse process of steel portal frames in fire, Journal of Constructional Steel Research, 2018, 150: 277-287.
[26] G. Q. Li, W. Ji, C. Y. Feng, Y. Wang, G. B. Lou. Experimental and numerical study on collapse modes of single-span steel portal frames under fire, Engineering Structures, 2021, 245: 112968.

[27] W. Ji, G. Q. Li, G. B. Lou. Early-warning methods for fire-induced collapse of single-span steel portal frames. Journal of Constructional Steel Research, 2022, 190(2): 107154.

[28] EN 1993-1-2, Design of steel structures, Part 1, 2: General Rules- Structure Fire Design, European Committee for Standardization (CEN), Brussels, 2005.

[29] GB50016, Code for fire protection design of buildings, China Architecture & Building Press, 2018.

[30] J. Jiang, G. Q. Li. Disproportionate collapse of 3D steel-framed structures exposed to various compartment fires. Journal of Constructional Steel Research, 2017, 138: 594-607.

[31] R. Sun, I W. Burgess, Z Huang, G Dong. Progressive failure modelling and ductility demand of steel beam-to-column connections in fire. Engineering Structures, 2015, 85(15): 66-78.

[32] G. Q. Li, W. Y. Wang, S. W. Chen. A simple approach for modeling fire-resistance of steel columns with locally damaged fire protection. Engineering Structures, 2009, 31: 617-622.

[33] G. B. Lou, C. H. Wang, J. Jiang, *et al*. Fire tests on full-scale steel portal frames against progressive collapse. Journal of Constructional Steel Research, 145(2018) 137-152.

[34] 07SG518-4, Design of Light Steel Portal Frames, China Building Standard Design and Research Institute, 2007.